Zeitschrift: Helvetica Physica Acta
Band: 42 (1969)
Heft: 3

Artikel: Residual interactions and properties of nuclear states in the lead region
Autor: Hadermann, J. / Alder, K.
DOI: https://doi.org/10.5169/seals-114079

Residual Interactions and Properties of Nuclear States in the Lead Region

by **J. Hadermann** and **K. Alder**
Institute of Theoretical Physics, University of Basel, Basel, Switzerland

(14. X. 68)

Abstract. Introducing a residual interaction with a spin-spin and a tensor part, energy levels and transition probabilities of the three single-closed shell nuclei Pb^{206}, Pb^{210}, Po^{210} have been computed and compared with experimental data. The parameters of the residual interaction potential are close to the values known from nucleon-nucleon scattering data and from deuteron theory.

1. Introduction

Many nuclear properties can be explained qualitatively with the shell model. However, for a detailed understanding of nuclear properties, residual interactions between the nucleons play a fundamental role. As a simple expression for the residual interaction pairing and quadrupole or delta forces have been considered. Recently more complex, 'realistic', potentials of the residual interaction, as the HAMADA-JOHNSTON [1] and the TABAKIN [2] potential reproducing nucleon-nucleon scattering data up to about 320 MeV have been introduced.

It is our aim to describe energies and properties of nuclear states with a phenomenological residual interaction which on the one hand is not as complex as the realistic potentials but on the other hand is a better approximation than the pairing or the delta force. For this reason we have chosen the simple deuteron potential and have investigated the influence of the spin-spin and the tensor part.

Effects of core excitation are not taken into account. It is well known [3, 4], that these effects become very important in medium heavy nuclei. They are, however, appreciably smaller for nuclei in the lead region and can be neglected to first order. Furthermore proton and neutron shells are here well separated.

We consider only nuclei in the lead region with two protons or neutrons (or holes) outside (inside) closed shells. Thus an exact diagonalization of the Hamiltonian is possible.

In section two a collection of properties of one and two-particle operators is given. In section three we discuss the residual interaction while in section four the nuclear Hamiltonian is introduced. Numerical results for the three nuclei Pb^{206}, Pb^{210} and Po^{210} are presented and discussed in section five. The last section deals mainly with the effects of core excitation.

2. Operator Relations

In the following we work with one and two-particle operators in the second quantization and give a brief summary of their properties[1]).

The creation and destruction operators for a single nucleon are denoted by a^+_{jm} and a_{jm}, respectively. The indices j and m are the total spin and the magnetic quantum number of the nucleon, where the index j includes implicitely all other quantum numbers.

It is convenient to define the following one-particle and two-particle operators:

$$A^+_{JM}(j_1\, j_2) = \sum_{m_1 m_2} (-)^{j_2 - m_2} \langle j_1\, m_1\, j_2 - m_2 \mid J\, M\rangle\, a^+_{j_1 m_1}\, a_{j_2 m_2} \tag{1}$$

and

$$B^+_{JM}(j_1\, j_2) = \frac{1}{\sqrt{1+\delta_{j_1 j_2}}} \sum_{m_1 m_2} \langle j_1\, m_1\, j_2\, m_2 \mid J\, M\rangle\, a^+_{j_1 m_1}\, a^+_{j_2 m_2},\ j_1 \geq j_2 \tag{2}$$

which transform as spherical tensors of order J. It is noted that $\sum_j (2\,j+1)^{1/2}\, A^+_{00}(j\,j)$ is the number operator for all nucleons and that the following symmetry relation is valid

$$B^+_{JM}(j_2\, j_1) = -\,(-)^{j_1+j_2+J}\, B^+_{JM}(j_1\, j_2)\,. \tag{3}$$

We get for the commutator of the two-particle operators

$$[B_{JM}(j_1\, j_2),\, B^+_{J'M'}(j'_1\, j'_2)] = \delta_{JJ'}\, \delta_{MM'}\, \delta_{j_1 j'_1}\, \delta_{j_2 j'_2} + \text{terms in } A^+_{LA}(j\, j')\,. \tag{4}$$

Since we are considering only systems with two nucleons outside the inert nuclear core, the states $B^+_{JM}(j_1\, j_2)\,|0\rangle$ form a complete basis. From equation (4) it follows that these states are orthogonal and normalized.

For the same reason we can substitute for the operator $A^+_{JM}(j_1\, j_2)$ the expression

$$\overline{A}^+_{JM}(j_1\, j_2) = (-)^{j_1+j_2+J} \sum_{\substack{J'M' \\ J''M'' \\ j}} (-)^{J''-M''} \sqrt{(2\,J'+1)\,(2\,J''+1)}\, \sqrt{(1+\delta_{j_1 j})\,(1+\delta_{j_2 j})}$$

$$\times \langle J'\, M'\, J'' - M'' \mid J\, M\rangle \begin{Bmatrix} J' & J'' & J \\ j_2 & j_1 & j \end{Bmatrix} B^+_{J'M'}(j_1\, j)\, B_{J''M''}(j\, j_2)\,. \tag{5}$$

Here the symmetry relation, equation (3), is used. Thus, it is possible to write all operators in terms of the two-particle operators $B^+_{JM}(j_1\, j_2)$. In particular this also holds for electromagnetic multipole operators [7].

3. The Potential of the Residual Interaction

The properties of the deuteron, especially the binding energy and the quadrupole moment, can only be explained if the interaction between the nucleons contains a spin-spin and a tensor part. Thus we assume the following form for the residual interaction

$$V(\boldsymbol{r}_1, \boldsymbol{r}_2) = V_0(\boldsymbol{r}_1, \boldsymbol{r}_2)\left[1 + a\,\boldsymbol{\sigma}_1\cdot\boldsymbol{\sigma}_2 + b\left(\frac{3\,(\boldsymbol{\sigma}_1\cdot\boldsymbol{r}_{12})\,(\boldsymbol{\sigma}_2\cdot\boldsymbol{r}_{12})}{r_{12}^2} - \boldsymbol{\sigma}_1\cdot\boldsymbol{\sigma}_2\right)\right] \tag{6}$$

[1]) See also References [5] and [6].

where the scalar potential $V_0(\boldsymbol{r}_1, \boldsymbol{r}_2)$ shall be of the form

$$V_0(\boldsymbol{r}_1, \boldsymbol{r}_2) = V_0 \frac{1}{r_1 r_2} e^{-\alpha r_{12}^2} \delta(\Omega_{12}) . \tag{7}$$

This special dependence on the coordinates is suggested by the success of similar computations with delta force or with surface delta interaction [8]. The angular dependence of these potentials has been retained, whereas the Gaussian radial dependence accounts for the finite range of the nuclear forces. (The radial distances are measured in units of oscillator lengths, i.e. $\sqrt{\hbar/M\,\omega_0}$ with $\hbar\,\omega_0 \simeq 41\ A^{-1/3}$ MeV.) As will be shown in the next section the parity-spin selection rule, which is exact for the two mentioned delta interaction potentials, is violated because of the finite range of the potential and is only approximately valid.

This simple residual interaction produces a correlation of the nucleons and consequently a strong configuration mixing. The delta function of the angular part will be expanded in spherical harmonics (see Appendix). The low multipoles of this expansion give rise to a correlation of the nucleons persisting at large angular distances. In particular the expansion contains terms which correspond to pairing forces and to quadrupole forces.

Four parameters appear in the expression of the residual interaction: (i) the potential depth V_0, (ii) the range α of the interaction, (iii) the relative strength a of the spin-spin part, and finally (iv) the relative magnitude b of the tensor part.

The potential depth V_0 is fitted by the energy difference between ground state and first excited state. For $a = b = .0$ the values of V_0 correspond to those of nucleon-nucleon scattering within 25 percent.

The energy spectrum of Pb^{206} is most sensitive to the choice of the three remaining parameters and this makes possible a reliable determination of α, a and b. The same set of parameters (α, a, b) can also be chosen for the two other nuclei.

As will be shown in section five the parameters $\alpha = 2.$, $a = .10$ and $b = .776$ give best agreement with experiment. The deuteron theory yields for comparison $a = .13$ and $b = .775$ [9, 10]. The parameter $\alpha = 2.$ corresponds to a range of the nuclear force of 1.72×10^{-13} cm. Nucleon-nucleon scattering data fitted by a Gaussian potential [11] give a range of 1.78×10^{-13} cm.

This good agreement between these values should not be taken too seriously. First, the parameters from nucleon-nucleon scattering and from deuteron theory can be varied considerably without changing essentially the fit of experimental data. It is also known [12] that the tensor part possesses a larger range than the scalar part. Secondly, a part of the effective nucleon-nucleon interaction has already been taken into account by the mean potential and enters through single-particle energies, which are taken from the experiment. Third, we do not expect that the interaction between free nucleons and those in nuclear matter are exactly the same.

The comparison between the fitted parameters and those obtained from experiment shows, however, that within our model the residual interaction, equation (6), represents a good assumption. It describes to a good approximation the lower-lying states of some nuclei in the lead region.

4. The Nuclear Hamiltonian

The Hamiltonian for the two nucleons outside a closed shell is given by

$$H = H_0 + H_R \tag{8}$$

where

$$H_0 = \sum_j \sqrt{2j+1}\, \varepsilon_j\, A^+_{00}(j\,j) \tag{9}$$

represents the effect of the mean nuclear potential containing the single-particle energies ε_j while

$$H_R = \sum_{\text{all } j\,m} \langle j_1\, m_1 \mid \langle j_2\, m_2 \mid V \mid j_1'\, m_1' \rangle \mid j_2'\, m_2' \rangle\, a^+_{j_1 m_1}\, a^+_{j_2 m_2}\, a_{j_2' m_2'}\, a_{j_1' m_1'} \tag{10}$$

describes the residual interaction between the two nucleons. The summations go over all configurations of the nucleons outside the closed shell. From the rotational invariance of the residual interaction it is convenient to introduce the quantity

$$\bar{G}_J(j_1\, j_2\, j_1'\, j_2') = \sum_{\text{all } m} \langle j_1\, m_1\, j_2\, m_2 \mid J\, M \rangle \langle j_1'\, m_1'\, j_2'\, m_2' \mid J\, M \rangle \langle j_1\, m_1 \mid \langle j_2\, m_2 \mid V \mid j_1'\, m_1' \rangle \mid j_2'\, m_2' \rangle . \tag{11}$$

Because of the Pauli principle only the antisymmetrized quantity

$$G_J(j_1\, j_2\, j_1'\, j_2') = \frac{1}{2} \left(\bar{G}_J(j_1\, j_2\, j_1'\, j_2') - (-)^{j_1+j_2+J}\, \bar{G}_J(j_2\, j_1\, j_1'\, j_2') \right) \tag{12}$$

contributes to the Hamiltonian. By using equation (5) the Hamiltonian H can be written

$$H = \sum_{JM} H_{JM} = \sum_{JM} \sum_{\substack{j_1 \geq j_2 \\ j_1' \geq j_2'}} \Big\{ (\varepsilon_{j_1} + \varepsilon_{j_2})\, \delta_{j_1 j_1'}\, \delta_{j_2 j_2'} + 2 \sqrt{(2 - \delta_{j_1 j_2})\, (2 - \delta_{j_1' j_2'})} \times G(j_1\, j_2\, j_1'\, j_2') \Big\}\, B^+_{JM}(j_1\, j_2)\, B_{JM}(j_1'\, j_2') . \tag{13}$$

As a result of the commutator relation (4) we can draw two immediate conclusions: First, the Hamiltonian decomposes in the various multipoles H_{JM}. Second, these multipole terms can be diagonalized separately by a single-particle transformation. The nuclear eigenstates can be written in the form

$$\bar{B}^+_{JM}(k) \mid 0 \rangle = \sum_{j_1 \geq j_2} C^J_{j_1 j_2, k}\, B^+_{JM}(j_1\, j_2) \mid 0 \rangle \tag{14}$$

where k numbers the states of spin J. The quantities $C^J_{j_1 j_2, k}$ are the elements of the unitary transformation matrix.

The magnitude and type of the configuration mixing is determined by the expression $G_J(j_1\, j_2\, j_1'\, j_2')$ which enters the residual interaction.

The calculation of $G_J(j_1\, j_2\, j_1'\, j_2')$ will be outlined in the appendix and we give here only the final result

$$\begin{aligned} G_J(j_1\, j_2\, j_1'\, j_2') = {} & \frac{1}{16\,\pi} \sqrt{(2j_1+1)\,(2j_2+1)\,(2j_1'+1)\,(2j_2'+1)}\, R^{n_1 l_1 n_1' l_1'}_{n_2 l_1 n_2' l_2'} \\ & \times \Big\{ (1 - \Delta)\,(1 + a + 2\,b) \begin{pmatrix} j_1 & j_2 & J \\ 1/2 & 1/2 & -1 \end{pmatrix} \begin{pmatrix} j_1' & j_2' & J \\ 1/2 & 1/2 & -1 \end{pmatrix} \\ & - (-)^{l_2+l_2'+j_2+j_2'} (1 + (-)^{l_1+l_2+J}\, \Delta) \\ & \times [1 - a - 2\,b + (-)^{l_1+l_2+J}\, 2\,(b - a)] \begin{pmatrix} j_1 & j_2 & J \\ 1/2 & -1/2 & 0 \end{pmatrix} \begin{pmatrix} j_1' & j_2' & J \\ 1/2 & -1/2 & 0 \end{pmatrix} \Big\} \end{aligned} \tag{15}$$

where we have defined the radial matrix element by

$$R^{n_1 l_1 n_1' l_1'}_{n_2 l_2 n_2' l_2'} = V_0 \langle n_1 l_1 | \langle n_2 l_2 | \frac{1}{r_1 r_2} e^{-\alpha r_{12}^2} | n_1' l_1' \rangle | n_2' l_2' \rangle \tag{16}$$

and where the ratio

$$\Delta = R^{n_2 l_2 n_1' l_1'}_{n_1 l_1 n_2' l_2'} / R^{n_1 l_1 n_1' l_1'}_{n_2 l_2 n_2' l_2'} \tag{17}$$

is introduced. The simplicity of this expression is essentially a consequence of the delta force in the angular part of the residual interaction.

The factors $(1 - \Delta)$ and $(1 + (-)^{l_1+l_2+J} \Delta)$ in equation (15) ensue from the antisymmetrization (see equation (12)). They are very important if Δ is either exactly or approximately one. This holds for many matrix elements of the residual interaction and therefore an approximate spin-parity selection rule follows.

Let us consider first the special case $\Delta = 1$ where the function $G_J(j_1 j_2 j_1' j_2')$ reduces to

$$G_J(j_1 j_2 j_1' j_2') = -\frac{1}{16\pi} (-)^{l_2+l_2'+j_2+j_2'} \sqrt{(2j_1+1)(2j_2+1)(2j_1'+1)(2j_2'+1)}$$
$$\times (1 + (-)^{l_1+l_2+J}) R^{n_1 l_1 n_1' l_1'}_{n_2 l_2 n_2' l_2'} (1 - 3a) \begin{pmatrix} j_1 & j_2 & J \\ 1/2 & -1/2 & 0 \end{pmatrix} \begin{pmatrix} j_1' & j_2' & J \\ 1/2 & -1/2 & 0 \end{pmatrix}. \tag{18}$$

The residual interaction influences only nucleon pairs with total spin J and parity $(-)^J$. Since there is always spin-orbit splitting of the single-particle states in the shell model, many matrix elements of the Hamiltonian fulfill this selection rule. States of spin J with parity $(-)^J$ show a particularly strong configuration mixing and are lowered considerably in their energy with respect to the single-particle picture. This is more true for states with positive parity, because the configuration space is larger than for states with negative parity. Transition probabilities between the afore mentioned strongly correlated states are appreciably larger than the corresponding single-particle values. A certain analogy to the vibration model becomes apparent here. However, in contrast to the vibration model, magnetic dipole transitions are not forbidden and cross-over is not prohibited. The tensor force gives no contribution to the matrix elements with $\Delta = 1$. The spin-spin part has the opposite sign with respect to the scalar part. Since a is of the order of magnitude 1/10, this only gives a renormalization of V_0 compared to the case $a = .0$.

For $\Delta \neq 1$ we may get contributions to the Hamilton matrix violating the spin-parity selection rule. The tensor part contributes to the second term of equation (15) only for $(-)^{l_1+l_2+J} = -1$. The effects of the tensor and the spin-spin interaction cancel partially, as can be seen in the example of Figures 2 and 3.

5. Numerical Calculations

For the three nuclei $_{82}Pb^{206}$, $_{82}Pb^{210}$, $_{84}Po^{210}$ numerical calculations were performed. Some numerical results for $_{28}Ni^{58}$ are commented in the next section in the context of a short discussion of core excitation. Preliminary results for $a = b = .0$ have already been reported in reference [13].

The single-particle energies ε_j in the diagonal part of the Hamiltonian (15) have been extracted from other experimental data and are compiled in Table I.

Table I

The single-particle energies and configurations taken from experiment.

Nucleus	Configuration	Single-particle Energy ε_j in MeV
$_{83}Bi^{209}$ [a]	$h_{9/2}$	.0
	$f_{7/2}$	.90
	$i_{13/2}$	1.61
$_{82}Pb^{209}$ [b]	$g_{9/2}$	.0
	$i_{11/2}$	.77
	$j_{15/2}$	1.41
	$d_{5/2}$	1.56
$_{82}Pb^{207}$ [c]	$p_{1/2}$	.0
	$f_{5/2}$	.57
	$p_{3/2}$	.90
	$i_{13/2}$	1.64
	$f_{7/2}$	2.53

[a] Ref. [34] [b] Ref. [35] [c] Ref. [36]

After a canonical transformation

$$r_1 = \frac{1}{\sqrt{2}}(R + r_{12}) \quad r_2 = \frac{1}{\sqrt{2}}(R - r_{12})$$

the radial matrix elements $R^{n_1 l_1 n_1' l_1'}_{n_2 l_2 n_2' l_2'}$ can be expressed in a closed form. The numerical calculations were done as follows: For $a = b = .0$, the range parameter α is varied and then, with adjusted range parameter ($\alpha = 2.$), the parameters a and b have been varied. The potential depth V_0 has always been fitted by the energy difference between ground state and first excited state.

Table II

A comparison is made between experiment and theory for several reduced electric quadrupole transition probabilities (units are barns^2). The parameters of the calculations are $\alpha = 2.$, $a = .10$ and $b = .776$.

Nucleus	Transition	$B(E2)$	
		Theory	Experiment
Pb^{206} [a]	$2_0^+ \to 0_0^+$	$.840 \times 10^{-2}$	$\left(.270 \begin{smallmatrix} + .005 \\ - .009 \end{smallmatrix}\right) \times 10^{-1}$
Pb^{210} [b]	$4_0^+ \to 2_0^+$	$.165 \times 10^{-1}$	$.328 \times 10^{-1}$
	$6_0^+ \to 4_0^+$	$.117 \times 10^{-1}$	$.302 \times 10^{-1}$
Po^{210} [c]	$4_0^+ \to 2_0^+$	$.134 \times 10^{-1}$	$(.192 \pm .025) \times 10^{-1}$
	$6_{0i}^+ \to 4_0^+$	$.933 \times 10^{-2}$	$(.128 \pm .016) \times 10^{-1}$

[a] Ref. [19] [b] Ref. [21] [c] Ref. [22]

For the computation of the reduced electromagnetic transition probabilities the gyromagnetic ratio g_l of the orbital momentum was set equal to unity for protons and neutrons. Correspondingly the effective charge of neutrons was assumed to be one electron charge. Some papers quote an effective charge in the heavy elements which is about 15% larger.

Electric dipole transitions are strongly forbidden in our model, since the reduced matrix elements $\langle j \| \mathcal{M}(E1) \| j' \rangle$ between single-particle states vanish for all configurations given in Table I.

A few electric quadrupole transition probabilities can be compared with experimental data. They are compiled in Table II.

5.1. *The Lead Isotope Pb^{206}*

The lead isotope Pb^{206} offers an excellent opportunity to compare theory and experiment. On the one hand the level scheme is very well known; spins and parities of many states have been measured [14, 15]. On the other hand the calculations are very sensitive to a variation of the parameters α, a and b. This is in contrast to the other two nuclei considered.

In addition to the configurations given in Table I V. GILLET [16] mentions a further single-particle level $h_{9/2}$ at 3.47 MeV. However, for the lower-lying states in

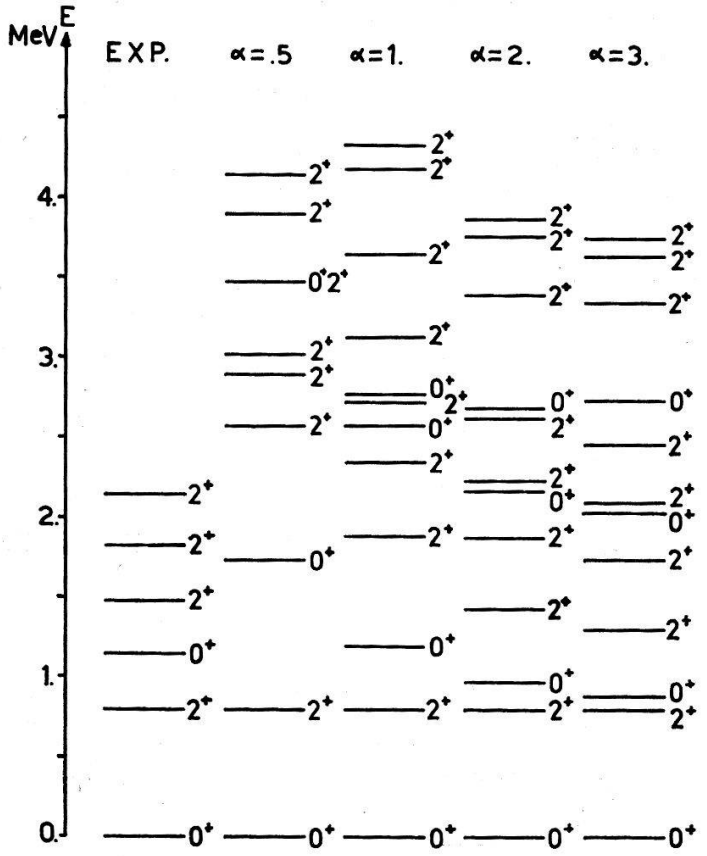

Figure 1

The variation for the states with spin 0^+ and 2^+ of Pb^{206} in function of the range parameter α is shown. The parameters a and b are chosen to be zero. The best agreement with experimental values is obtained for $\alpha = 2.$.

Pb^{206} the inclusion of this single-particle state essentially gives rise to a renormalization of the potential depth V_0 by about ten percent.

For $a = b = .0$ Figure 1 shows the variation of the states with spin 0^+ and 2^+ in function of the range parameter. The best fit is obtained with the parameter $\alpha = 2.$ corresponding to an interaction range of 1.72×10^{-13} cm, i.e. approximately a quarter of the nuclear radius. Figure 4 shows the complete level scheme for this set of parameters.

The influence of the spin-spin and the tensor part of the residual interaction has been investigated (see Figures 2 and 3) with a fixed value of the range ($\alpha = 2.$). The spin-spin interaction lowers most energy levels considerably. The effect of the tensor interaction is less marked since the matrix element of the tensor part often

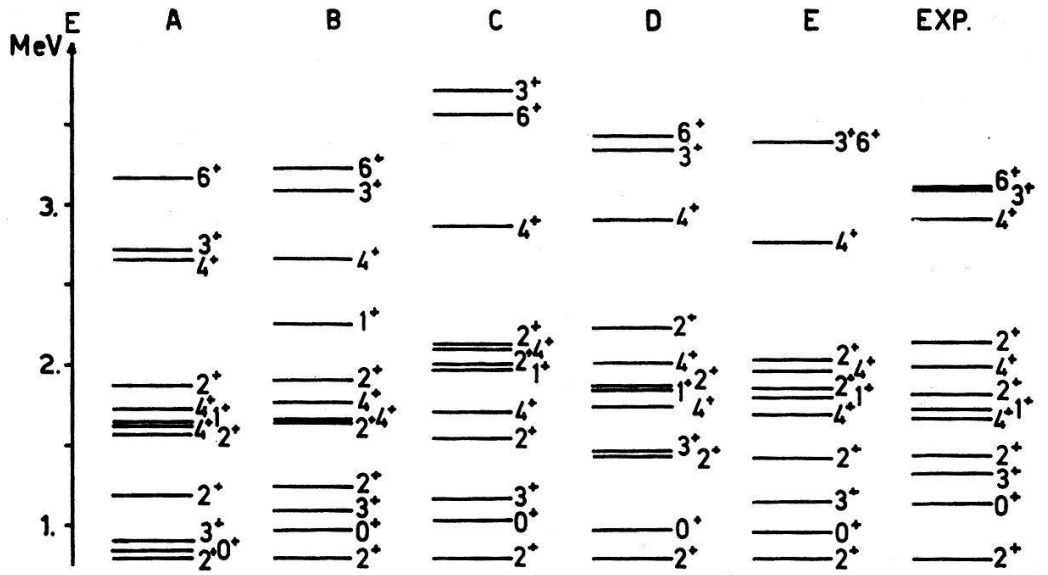

Figure 2

For various values of a and b theory and experiment are compared for states with positive parity in Pb^{206}. The range parameter is chosen to be $\alpha = 2.$. The parameters V_0, a and b are as follows: Calculation A) $V_0 = .321$ MeV, $a = .13$, $b = .0$; B) $V_0 = .212$ MeV, $a = .0$, $b = .775$; C) $V_0 = .446$ MeV, $a = .13$, $b = .775$; D) $V_0 = .183$ MeV, $a = .0$, $b = .0$; E) $V_0 = .355$ MeV, $a = .10$, $b = .776$. The introduction of a spin-spin and a tensor interaction yields an appreciable improvement.

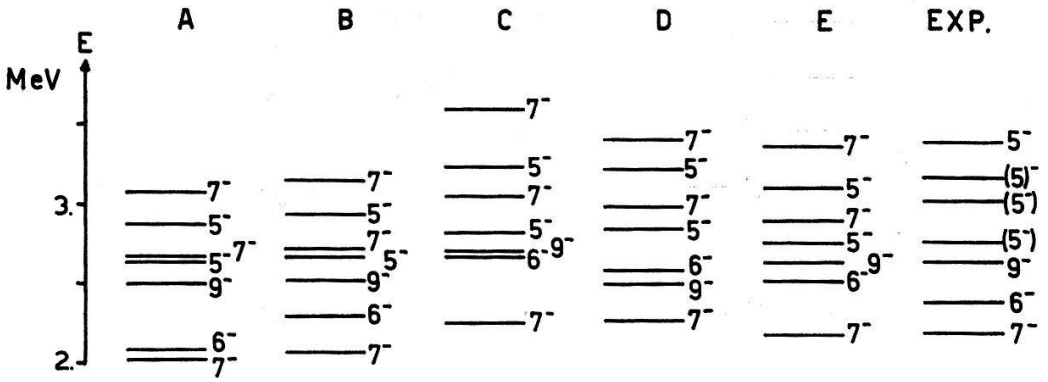

Figure 3

For several values of a and b the variation of the negative parity states in Pb^{206} is shown and a comparison with experimental data is made. The parameters are the same as in Figure 2.

vanishes. In Figures 2 and 3 it can easily be seen that the influence of the spin-spin and the tensor interaction cancel each other partially. The ranges in which the parameters a and b can reasonably be varied lie close to the deuteron values. Provided the potential depth V_0 is chosen in the order of magnitude of the values of nucleon-nucleon scattering, a ground state of spin 2^+ results for larger values of a and b ($a \gtrsim .19$ and (or) $b \gtrsim .8$). Only for values of V_0 which are some powers of magnitude larger the ground state has spin 0^+.

The mean square deviation of the calculated energy levels from experiment has the smallest value for the set of parameters $a = .10$ and $b = .776$. The potential depth is fitted by $V_0 = .355$ MeV. This is the same order of magnitude as the values extracted from scattering experiments.

Figure 4 illustrates clearly that by introducing a spin-spin and a tensor term in the residual interaction the level scheme of Pb^{206}, particularly also the sequence of the levels, can be well explained. The 3^- state at 2.35 MeV is known to be an octupole vibration and is thus not accounted for in our model. For states above 3.5 MeV our model becomes inadequate. Further single-particle configurations should be included. Also the effects of core excitations may essentially contribute. For $a = b = .0$ the interaction energy of the nucleon pair in the ground state is $-.512$ MeV, while for $a = .10$, $b = .776$ the corresponding value is $-.906$ MeV. It may be noted that the value of the interaction energy lies in the same order of magnitude as the Q-value of the reaction $Pb^{208}(d, t)Pb^{207}$, $Q = -1.13 \pm .01$ MeV [17].

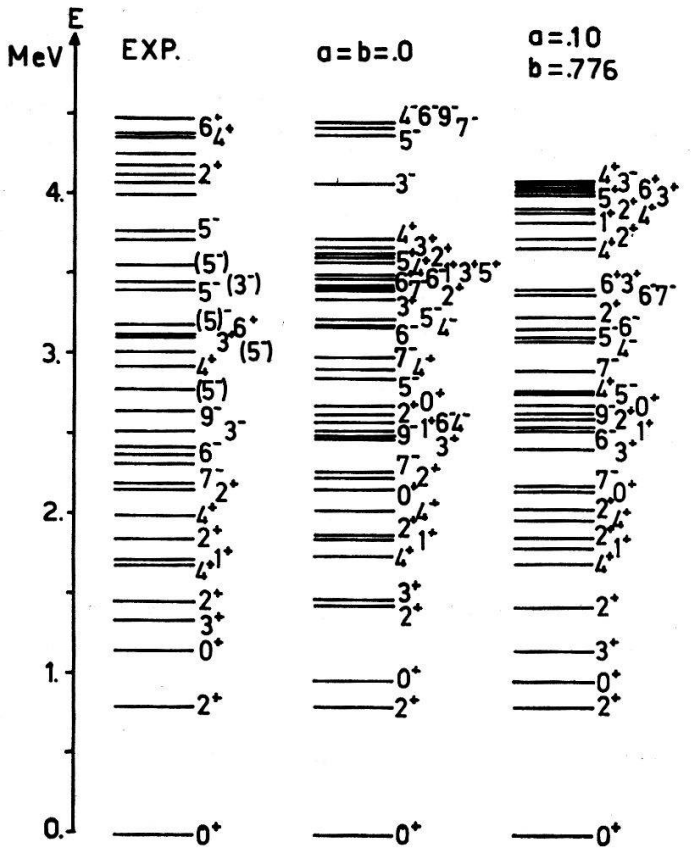

Figure 4

The entire level scheme for Pb^{206} with $a = b = .0$ and $a = .10$, $b = .776$ is compared with experimental data. The range parameter is chosen to be $\alpha = 2..$

Table III

For $\alpha = 2.$ some reduced transition probabilities in Pb^{206} are given (units are barns^2 for $E2$ transitions and $(e\,\hbar/2\,M\,c)^2$ for $M1$ transitions). The parameters a and b are varied.

Transition	$\sigma\lambda$	$a = b = .0$	$a = .13$ $b = .0$	$a = .0$ $b = .775$	$a = .13$ $b = .775$	$a = .10$ $b = .776$
$2_0^+ \to 0_0^+$	$E2$	$.913 \times 10^{-2}$	$.936 \times 10^{-2}$	$.918 \times 10^{-2}$	$.771 \times 10^{-2}$	$.840 \times 10^{-2}$
$2_1^+ \to 0_0^+$	$E2$	$.174 \times 10^{-1}$	$.177 \times 10^{-1}$	$.174 \times 10^{-1}$	$.148 \times 10^{-1}$	$.160 \times 10^{-1}$
$2_1^+ \to 2_0^+$	$E2$	$.449 \times 10^{-2}$	$.355 \times 10^{-2}$	$.410 \times 10^{-2}$	$.552 \times 10^{-2}$	$.512 \times 10^{-2}$
	$M1$	.594	.838	.511	$.222 \times 10^{-2}$	$.786 \times 10^{-1}$
$2_2^+ \to 2_0^+$	$E2$	$.184 \times 10^{-1}$	$.190 \times 10^{-1}$	$.187 \times 10^{-1}$	$.137 \times 10^{-1}$	$.166 \times 10^{-1}$
	$M1$	$.489 \times 10^{-1}$	$.529 \times 10^{-1}$	.124	$.134 \times 10^{1}$	.595
$2_2^+ \to 2_1^+$	$E2$	$.339 \times 10^{-3}$	$.124 \times 10^{-3}$	$.217 \times 10^{-3}$	$.132 \times 10^{-2}$	$.683 \times 10^{-3}$
	$M1$	$.569 \times 10^{1}$	$.478 \times 10^{1}$	$.501 \times 10^{1}$	$.565 \times 10^{1}$	$.542 \times 10^{1}$
$4_0^+ \to 2_0^+$	$E2$	$.359 \times 10^{-2}$	$.794 \times 10^{-2}$	$.111 \times 10^{-2}$	$.759 \times 10^{-2}$	$.626 \times 10^{-2}$
$4_0^+ \to 2_1^+$	$E2$	$.169 \times 10^{-1}$	$.159 \times 10^{-2}$	$.607 \times 10^{-2}$	$.822 \times 10^{-2}$	$.918 \times 10^{-2}$
$5_0^- \to 6_0^-$	$E2$	$.108 \times 10^{-1}$	$.106 \times 10^{-1}$	$.945 \times 10^{-2}$	$.719 \times 10^{-2}$	$.682 \times 10^{-2}$
	$M1$	$.612 \times 10^{1}$	$.118 \times 10^{2}$	$.976 \times 10^{1}$	$.188 \times 10^{2}$	$.133 \times 10^{2}$

In Table III some calculated reduced transition probabilities are compiled for various parameters a and b. The electric quadrupole transitions vary slowly with a and b. As expected a larger variation of the magnetic dipole transitions is observed. These calculated values deviate from the single-particle unit [18] up to a factor of ten. The reduced quadrupole transition probability between ground state and first excited state has been measured and is greater by a factor of three compared with the calculated value (see Table II). Furthermore the branching ratio for the decay of state 2_1^+ has been measured [20] and the following ratio of the $M1$ and $E2$ reduced transition probabilities for the transition $2_1^+ \to 2_0^+$ can be extracted

$$R = \frac{B(M1)}{B(E2)} = 8.50 \left(\frac{e\hbar}{2\,M\,c\,b}\right)^2.$$

Here too, the set of parameters $a = .10$, $b = .776$ gives best agreement namely $R = 15.4\ (e\,\hbar/2\,M\,c\,b)^2$. The strong variation of R with the parameters a and b is shown in Table IV.

Table IV

The variation of the ratio $B\,(M1)/B\,(E2)$ in units of $(e\,\hbar/2\,M\,c\,b)^2$ for the transition $2_1^+ \to 2_0^+$ in Pb^{206} is given for several values of a and b.

	$B\,(M1)/B\,(E2)$
$a = b = .0$	$.132 \times 10^3$
$a = .13,\ b = .0$	$.236 \times 10^3$
$a = .0,\ b = .775$	$.125 \times 10^3$
$a = .13,\ b = .775$	.402
$a = .10,\ b = .776$	$.154 \times 10^2$
Experiment	$.850 \times 10^1$

5.2. *The Lead Isotope Pb^{210}*

Comparatively little information exists on the energy levels of Pb^{210}. The position of the energy levels changes only slightly with variation of the range parameter α. This behaviour is shown in Figure 5. Similar results are also obtained if a spin-spin and a tensor interaction are introduced. In Figure 6 the calculated level scheme with the parameters $\alpha = 2.$, $a = .10$ and $b = .776$ is compared with experimental data [21]. Due to the lack of experimental results it is not possible to determine a unique set of parameters. As a common feature in all calculations the lowest states of spin 4^+ and 6^+ lie too low. This results from the neglect of core excitations. The state 3^- at 1.9 MeV is a strong configuration mixture in which the wave function of the configuration $(g_{9/2}, j_{15/2})_{3^-}$ lying at 2.3 MeV gives the largest contribution.

The interaction energy E_I of the nucleon pair in the ground state is not sensitive to the parameters α, a and b. One obtains $E_I = -.988$ MeV. This result can be compared with the Q-value of the reaction $Pb^{208}(d, p)Pb^{209}$ which amounts to $Q = -1.70 \pm .01$ MeV [17].

The reduced electric quadrupole probabilities for the transitions $4_0^+ \to 2_0^+$ and $6_0^+ \to 4_0^+$ has been extracted from the measured life times. As can be seen in Table II the theoretical and experimental values agree to within a factor of 2.5. Other calculated transition probabilities for which experimental information lacks are given in Table V. The electric quadrupole probabilities vary, as the energy levels, very slowly with the parameters α, a and b.

Table V

Some reduced transition probabilities for Pb^{210} are compiled (units are the same as in table III). The parameters are $\alpha = 2.$, $a = .10$ and $b = .776$. The values are only very little sensitive to the choice of the parameters.

Transition	$\sigma\lambda$	$B(\sigma\lambda)$	Transition	$\sigma\lambda$	$B(\sigma\lambda)$
$2_0^+ \to 0_0^+$	$E2$	$.117 \times 10^{-1}$	$2_1^+ \to 2_0^+$	$E2$	$.155 \times 10^{-2}$
$2_1^+ \to 0_0^+$	$E2$	$.153 \times 10^{-4}$		$M1$	$.642 \times 10^{-2}$
$2_2^+ \to 0_0^+$	$E2$	$.567 \times 10^{-2}$	$2_2^+ \to 2_0^+$	$E2$	$.110 \times 10^{-1}$
				$M1$	$.987 \times 10^{-1}$
$2_0^+ \to 4_0^+$	$E2$	$.296 \times 10^{-1}$	$4_2^+ \to 4_0^+$	$E2$	$.869 \times 10^{-2}$
$2_1^+ \to 4_0^+$	$E2$	$.700 \times 10^{-3}$		$M1$	$.406 \times 10^{-1}$
$2_2^+ \to 4_0^+$	$E2$	$.465 \times 10^{-2}$	$4_3^+ \to 4_0^+$	$E2$	$.594 \times 10^{-2}$
				$M1$	$.656 \times 10^{-1}$

5.3. *The Polonium Isotope Po^{210}*

The experimental situation with Po^{210} is essentially the same as with Pb^{210}, only a few energy levels and their spins have been measured [22]. For $a = b = .0$ the position of the energy levels is insensitive to the choice of the range parameter α. The results of our calculation for $\alpha = 2.$ are given in Figure 7, where the variation of the level scheme with the parameters a and b is illustrated. However, the states which can be compared with experimental data are not sensitive to a variation of a and b. The state at 1.48 MeV can be associated with spin and parity 6^+. The states at 2.91 MeV and 3.03 MeV are believed to have spin and parity 5^- and 4^-, respectively.

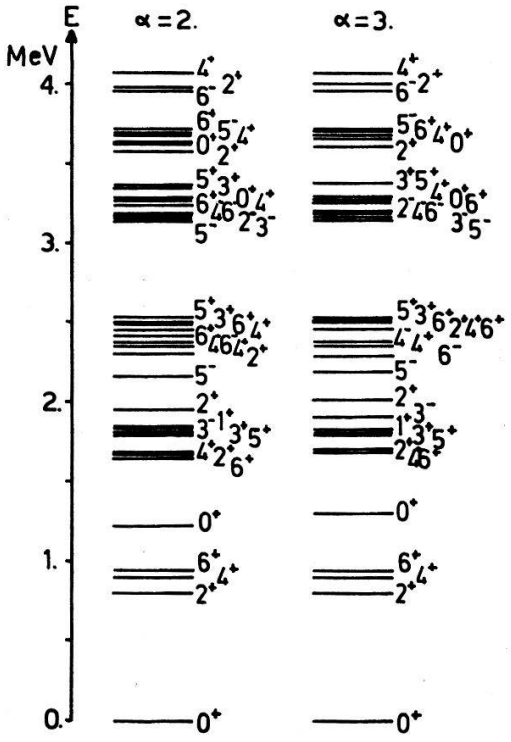

Figure 5

The level scheme of Pb^{210} is illustrated. It is shown that the positions of the levels are not sensitive to a variation of the range parameter α for $a = b = .0$.

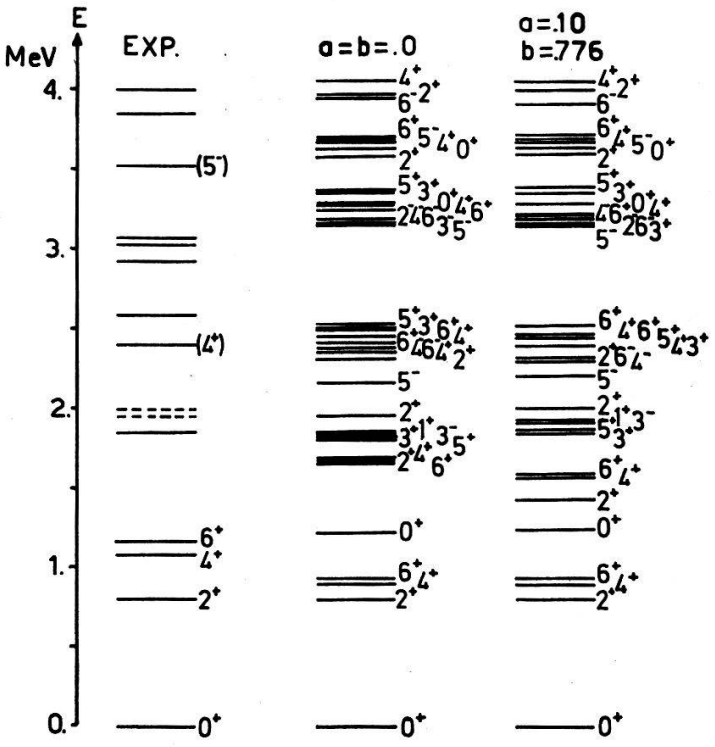

Figure 6

The energy spectrum of Pb^{210}. For the range parameter $\alpha = 2.$ calculations with $a = b = .0$ and $a = .10$, $b = .776$ are compared with experimental data. The scarce experimental information does not allow to decide between the two calculated level schemes.

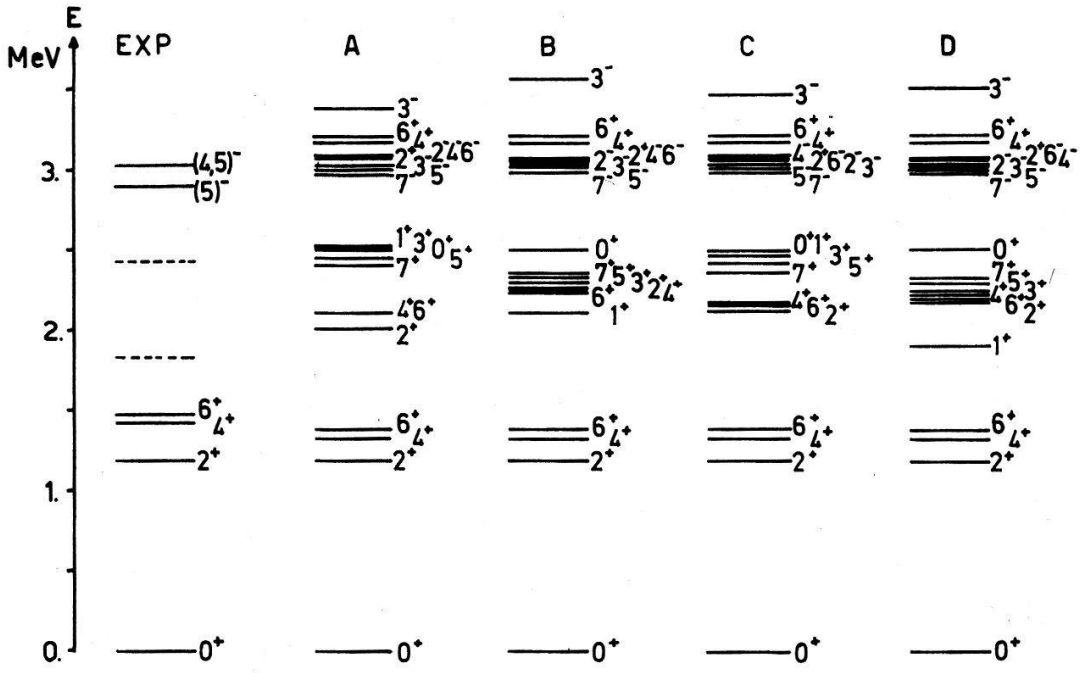

Figure 7

The energy spectrum of Po^{210}. A comparison is made between experiment and theory for various values of the parameters a and b. The range parameter is chosen to be $\alpha = 2.$. Most states are not sensitive to a variation of the parameters a and b. The parameters V_0, a and b are as follows: Calculation A) $V_0 = .184$ MeV, $a = .10$, $b = .776$; B) $V_0 = .128$ MeV, $a = b = .0$; C) $V_0 = .128$ MeV, $a = .0$, $b = .775$; D) $V_0 = .211$ MeV, $a = .13$, $b = .0$.

Compared to the pure single-particle picture the ground state of Po^{210} is lowered by 1.46 MeV by the residual interaction. This value is again not sensitive on the values of the parameters a and b.

In Table II reduced transition probabilities of the decays of the states 4_0^+ and 6_0^+ are compared with experimental values extracted from lifetime measurements [22]. The agreement is very good although the theoretical values are somewhat too small. For various parameters a and b some further reduced transition probabilities are

Table VI

Some reduced transition probabilities in Po^{210} (units are the same as in table III) are given for $\alpha = 2.$ and for several values of a and b.

Transition	$\sigma\lambda$	$a = b = .0$	$a = .0$ $b = .775$	$a = .13$ $b = .0$	$a = .10$ $b = .776$
$2_0^+ \to 0_0^+$	$E2$	$.107 \times 10^{-1}$	$.107 \times 10^{-1}$	$.107 \times 10^{-1}$	$.107 \times 10^{-1}$
$4_0^+ \to 2_0^+$	$E2$	$.134 \times 10^{-1}$	$.134 \times 10^{-1}$	$.134 \times 10^{-1}$	$.134 \times 10^{-1}$
$6_0^+ \to 4_0^+$	$E2$	$.931 \times 10^{-2}$	$.932 \times 10^{-2}$	$.931 \times 10^{-2}$	$.933 \times 10^{-2}$
$4_1^+ \to 4_0^+$	$E2$	$.190 \times 10^{-3}$	$.188 \times 10^{-3}$	$.189 \times 10^{-3}$	$.186 \times 10^{-3}$
	$M1$	$.161 \times 10^{-1}$	$.190 \times 10^{-1}$	$.176 \times 10^{-1}$	$.220 \times 10^{-1}$
$5_0^+ \to 6_0^+$	$E2$	$.124 \times 10^{-4}$	$.122 \times 10^{-4}$	$.123 \times 10^{-4}$	$.121 \times 10^{-4}$
	$M1$	$.656 \times 10^{-1}$	$.785 \times 10^{-1}$	$.721 \times 10^{-1}$	$.914 \times 10^{-1}$
$4_0^- \to 5_0^-$	$E2$	$.820 \times 10^{-2}$	$.836 \times 10^{-2}$	$.823 \times 10^{-2}$	$.826 \times 10^{-2}$
	$M1$	$.660 \times 10^{2}$	$.660 \times 10^{2}$	$.660 \times 10^{2}$	$.660 \times 10^{2}$

compiled in Table VI. Only a very weak variation of the quantities $B(\sigma\lambda)$ is seen. However, some of the values of $B(M1)$ deviate appreciably from the Weisskopf unit.

Furthermore F. SCHIMA et al. [22] quote the multipole orders of some transitions. Especially the state 4_0^- decays by an electric dipole transition which in our model is strongly forbidden. A finite transition probability may be explained by the influence of higher-lying single-particle states (e.g. a $h_{11/2}$ level) and by effects of core excitations. However, electric dipole transition probabilities are small. The experimental branching ratio at the decay of the state 4_0^- gives

$$\frac{B\,(M1,\,4_0^- \to 5_0^-)}{B\,(E1,\,4_0^- \to 4_0^+)} = 2.8 \times 10^2 \,\frac{1}{b}\left(\frac{e\hbar}{2\,Mc}\right)^2 .$$

6. Conclusions

It has been shown that the positions of most energy levels and some properties of nuclear states in the three nuclei Pb^{206}, Pb^{210}, Po^{210} can be described very well by a phenomenological residual interaction between the valence nucleons. The agreement with the experimental data is appreciable better than the calculations with a Gaussian interaction [23], a surface delta interaction [24] or a Tabakin interaction [25]. Recent calculations of W. W. TRUE [26] using a singlet-even force agree better with our results.

We would like to point out that apart from the potential parameter V_0 only three free parameters enter the calculation through the residual interaction (6). These parameters can be chosen the same in all three nuclei. They lie close to the values obtained from nucleon-nucleon scattering and deuteron theory.

The potential parameter V_0 is fitted by the energy difference between ground state and first excited state. It is particularly sensitive to the special form of the residual interaction. Therefore V_0 is different in all three nuclei. We may think of two further reasons for the relatively large variation of V_0. First, it is inevitable that the first excited state has an admixed collective part from core excitations which we have neglected. It may be assumed that this admixture is different for all three nuclei. Second, it is noted that the number of single-particle configurations considered is different in all three nuclei. We have compiled the various values for the potential depth V_0 in Table VII. If we choose $a = b = .0$, the parameter V_0 can be compared with data extracted from nucleon-nucleon scattering [27]. Assuming a $1/A$ dependence of the coupling constant on the atomic number (in analogy to the pairing force) we get $V_{NN} = 31.7/\mathrm{A\,MeV}$. It is noted that V_{NN} and V_0 (for $a = b = .0$) deviate by less than 25 percent. For $a = .10$, $b = .776$ the values of V_0 are larger for reasons discussed in Section 4.

Now we shall shortly comment the effect of core excitations. For nuclei in the lead region these effects are believed to be small since in our model the residual interaction between the nucleons describes the positions and properties of the states very well. However, they are noticeable in all three nuclei[2]). It has be shown [28], that a weak

[2]) In medium heavy nuclei the assumption of an inert nuclear core is no longer justified. Calculations for Ni^{58} have shown that the two valence nucleons cannot explain the large energy difference $\Delta E > 1$ MeV between first excited and higher lying states. Also the calculated transition probability $B\,(E2,\,2_0^+ \to 0_0^+)$ is too small by more than a factor of ten. This indicates that core excitations may become very important.

Table VII

The fitted values of V_0 (in MeV) for the potential depth are compiled. The range parameter is $\alpha = 2..$ For $a = b = .0$ V_0 can be compared with the values from nucleon-nucleon scattering.

Nucleus	$a = .10,\ b = .776$	$a = b = .0$	Nucleon-nucleon scattering
Pb^{206}	.355	.183	.154
Pb^{210}	.233	.117	.151
Po^{210}	.184	.128	.151

coupling of the outer nucleons to the nuclear core corresponds in first approximation to a quadrupole force between the valence nucleons. This quadrupole force causes a further increase in configuration mixing and thus particularly an increase of most transition probabilities. In our model the transition probabilities are somewhat too small (see also Table II). Particularly the first excited state of spin 2^+ is lowered in energy. Thus a larger energy difference between this state and the higher lying states is obtained. In this way the relatively large energy difference between the states 2_0^+ and 4_0^+ in Pb^{210} and the much smaller one in Po^{210} can be explained. Introducing core excitations it should be possible to account also for the states above 4 MeV in Pb^{206}. A more detailed investigation considering excitation of nucleon pairs from the nuclear core will be published in a separate paper [29].

One of the authors (J. H.) gratefully acknowledges a grant from the Swiss National Science Foundation.

7. Mathematical Appendix

We want to outline briefly the calculation of the unsymmetrized quantity $\overline{G}_J(j_1\, j_2\, j_1'\, j_2')$, equation (11), and of the antisymmetrized quantity $G_J(j_1\, j_2\, j_1'\, j_2')$, equation (12).

We transform the angular part of the nuclear wave function from j–j to L–S coupling [30] and thus get

$$\begin{aligned}\overline{G}_J(j_1\, j_2\, j_1'\, j_2') = &\sqrt{(2\,j_1+1)\,(2\,j_2+1)\,(2\,j_1'+1)\,(2\,j_2'+1)} \\ &\times \sum_{\substack{L\,\Lambda \\ L'\,\Lambda' \\ S\,\Sigma \\ S'\,\Sigma'}} \sqrt{(2\,L+1)\,(2\,L'+1)\,(2\,S+1)\,(2\,S'+1)} \\ &\times \langle L\,\Lambda\,S\,\Sigma \mid J\,M\rangle\,\langle L'\,\Lambda'\,S'\,\Sigma' \mid J\,M\rangle \\ &\times \begin{Bmatrix} l_1 & l_2 & L \\ s_1 & s_2 & S \\ j_1 & j_2 & J \end{Bmatrix} \begin{Bmatrix} l_1' & l_2' & L' \\ s_1' & s_2' & S' \\ j_1' & j_2' & J \end{Bmatrix} \langle S\,\Sigma \mid \langle L\,\Lambda \mid V \mid L'\,\Lambda'\rangle \mid S'\,\Sigma'\rangle\,. \end{aligned} \tag{A.1}$$

For the explicit calculation of the matrix element of the residual interaction, we specify the wave functions of the nucleons [31] in the mean potential by

$$|\,j\,m\rangle = N \sum_{\lambda\,\sigma} \langle l\,\lambda\,s\,\sigma \mid j\,m\rangle\, Y_{l\,\lambda}\, \chi_\sigma\, r^l\, e^{-1/2\,r^2}\, {}_1F_1\,(-n,\, l+{}^3/_2,\, r^2) \tag{A.2}$$

where N is a normalizing factor and χ_σ the nucleon spinor.

A radial matrix element can be extracted by writing

$$\langle S\,\Sigma \mid \langle L\,\Lambda \mid V \mid L'\,\Lambda' \rangle \mid S'\,\Sigma' \rangle = R^{n_1 l_1 n_1' l_1'}_{n_2 l_2 n_2' l_2'} \langle S\,\Sigma \mid \langle L\,\Lambda \mid V' \mid L'\,\Lambda' \rangle \mid S'\,\Sigma' \rangle . \quad \text{(A.3)}$$

The scalar part of the interaction (6) can be expanded into a multipole series

$$\delta(\Omega_{12}) = \sum_{l\,m} (-)^m\, Y_{l\,-m}(1)\, Y_{l\,m}(2) . \quad \text{(A.4)}$$

We get for the matrix element the following result

$$\langle S\,\Sigma \mid \langle L\,\Lambda \mid \delta(\Omega_{12}) \mid L'\,\Lambda' \rangle \mid S'\,\Sigma' \rangle = \delta_{S\,S'}\,\delta_{\Sigma\,\Sigma'}\,\delta_{L\,L'}\,\delta_{\Lambda\,\Lambda'}\,\frac{1}{4\pi}$$
$$\times \sqrt{(2\,l_1+1)\,(2\,l_2+1)\,(2\,l_1'+1)\,(2\,l_2'+1)}\begin{pmatrix} l_1 & l_2 & L \\ 0 & 0 & 0 \end{pmatrix}\begin{pmatrix} l_1' & l_2' & L \\ 0 & 0 & 0 \end{pmatrix} . \quad \text{(A.5)}$$

The matrix element for the spin-spin interaction is similarly given by

$$\langle S\,\Sigma \mid \langle L\,\Lambda \mid \boldsymbol{\sigma}_1 \cdot \boldsymbol{\sigma}_2\, \delta(\Omega_{12}) \mid L'\,\Lambda' \rangle \mid S'\,\Sigma' \rangle = -\,(-)^S\,\delta_{S\,S'}\,\delta_{\Sigma\,\Sigma'}\,\delta_{\Lambda\,\Lambda'}\,\frac{3}{4\pi}\,\frac{1}{2\,S+1}$$
$$\times \sqrt{(2\,l_1+1)\,(2\,l_2+1)\,(2\,l_1'+1)\,(2\,l_2'+1)}\begin{pmatrix} l_1 & l_2 & L \\ 0 & 0 & 0 \end{pmatrix}\begin{pmatrix} l_1' & l_2' & L' \\ 0 & 0 & 0 \end{pmatrix} . \quad \text{(A.6)}$$

The tensor operator may be expanded in the following way

$$\delta(\Omega_{12})\,\frac{3\,(\boldsymbol{\sigma}_1 \cdot \boldsymbol{r}_{12})\,(\boldsymbol{\sigma}_2 \cdot \boldsymbol{r}_{12})}{r_{12}^2} = 3 \sum_{\substack{l\,\lambda \\ l'\,\lambda' \\ l''\,\lambda'' \\ \mu\,\mu'}} (-)^\lambda\,(2\,l+1)\,\sqrt{(2\,l'+1)\,(2\,l''+1)}\begin{pmatrix} 1 & l & l' \\ 0 & 0 & 0 \end{pmatrix}\begin{pmatrix} 1 & l & l'' \\ 0 & 0 & 0 \end{pmatrix}$$
$$\times \begin{pmatrix} 1 & l & l' \\ -\,\mu & -\,\lambda & -\,\lambda' \end{pmatrix}\begin{pmatrix} 1 & l & l'' \\ -\,\mu' & \lambda & -\,\lambda'' \end{pmatrix} \sigma_{1\,\mu}\,\sigma_{2\,\mu'}\, Y_{l'\,\lambda'}(1)\, Y_{l''\,\lambda''}(2) . \quad \text{(A.7)}$$

With the help of relations between various Wigner symbols [30] and the useful formula [32]

$$\sum_{l'} (2\,l'+1)\begin{pmatrix} l'' & l' & K \\ 0 & 0 & 0 \end{pmatrix}\begin{pmatrix} l_1 & l_1' & l' \\ 0 & 0 & 0 \end{pmatrix}\begin{Bmatrix} l_1 & l_1' & l' \\ l_2 & l_2' & l'' \\ L & L' & K \end{Bmatrix} = \sum_{\mu} \begin{pmatrix} l_1 & l_2 & L \\ 0 & \mu & -\mu \end{pmatrix}\begin{pmatrix} l_1' & l_2' & L' \\ 0 & -\mu & \mu \end{pmatrix}$$
$$\times \begin{pmatrix} l_2 & l_2' & l'' \\ \mu & -\mu & 0 \end{pmatrix}\begin{pmatrix} L & L' & K \\ -\mu & \mu & 0 \end{pmatrix} \quad \text{(A.8)}$$

we get for the tensor part of the matrix element

$$\langle S\,\Sigma \mid \langle L\,\Lambda \mid \delta(\Omega_{12}) \left(\frac{3\,(\boldsymbol{\sigma}_1 \cdot \boldsymbol{r}_{12})\,(\boldsymbol{\sigma}_2 \cdot \boldsymbol{r}_{12})}{r_{12}^2} - \boldsymbol{\sigma}_1 \cdot \boldsymbol{\sigma}_2 \right) \mid L'\,\Lambda' \rangle \mid S'\,\Sigma' \rangle = (-)^\Sigma\,\delta_{S\,S'}\,\delta_{S\,1}\,\frac{\sqrt{30}}{2\pi}$$
$$\times \sqrt{(2\,L+1)\,(2\,L'+1)\,(2\,l_1+1)\,(2\,l_2+1)\,(2\,l_1'+1)\,(2\,l_2'+1)}$$
$$\times \begin{pmatrix} l_1 & l_2 & L \\ 0 & 0 & 0 \end{pmatrix}\begin{pmatrix} l_1' & l_2' & L' \\ 0 & 0 & 0 \end{pmatrix}\begin{pmatrix} L & 2 & L' \\ 0 & 0 & 0 \end{pmatrix} \sum_{\varkappa} (-)^\varkappa \begin{pmatrix} S & 2 & S' \\ -\,\Sigma & \varkappa & \Sigma' \end{pmatrix}\begin{pmatrix} L & 2 & L' \\ -\,\Lambda & -\,\varkappa & \Lambda' \end{pmatrix} . \quad \text{(A.9)}$$

For further calculation we may mention the following relation [33]

$$\begin{Bmatrix} l_1 & l_2 & L \\ s_1 & s_2 & S \\ j_1 & j_2 & J \end{Bmatrix} \begin{Bmatrix} l_1' & l_2' & L \\ s_1' & s_2' & S \\ j_1' & j_2' & J \end{Bmatrix} = \sum_{\substack{\gamma_1 \gamma_2 \\ \delta \varepsilon}} (-)^{s_2+j_1'-L-\delta} (2\gamma_1+1)(2\gamma_2+1)(2\delta+1)(2\varepsilon+1)$$
$$\times \begin{Bmatrix} j_1 & l_1 & s_1 \\ j_2 & \varepsilon & \delta \\ J & j_1' & j_2' \end{Bmatrix} \begin{Bmatrix} j_1' & l_1' & s_1' \\ \varepsilon & l_2' & \gamma_2 \\ l_1 & L & l_2 \end{Bmatrix} \begin{Bmatrix} j_2 & l_2 & s_2 \\ \varepsilon & \gamma_2 & l_2' \\ \delta & s_1' & \gamma_1 \end{Bmatrix} \begin{Bmatrix} j_2' & l_2' & s_2' \\ s_1 & s_2 & S \\ \delta & \gamma_1 & s_1' \end{Bmatrix}. \tag{A.10}$$

After a lengthy but straight-forward calculation we get the simple expression

$$G_J^S(j_1 j_2 j_1' j_2') = \frac{1}{16\pi} \sqrt{(2j_1+1)(2j_2+1)(2j_1'+1)(2j_2'+1)}\, R^{n_1 l_1 n_1' l_1'}_{n_2 l_2 n_2' l_2'}$$
$$\times \Big\{ (1-\Delta) \begin{pmatrix} j_1 & j_2 & J \\ 1/2 & 1/2 & -1 \end{pmatrix} \begin{pmatrix} j_1' & j_2' & J \\ 1/2 & 1/2 & -1 \end{pmatrix}$$
$$- (-)^{l_2+l_1'+j_2+j_2'} (1+(-)^{l_1+l_2+J}\Delta) \begin{pmatrix} j_1 & j_2 & J \\ 1/2 & -1/2 & 0 \end{pmatrix} \begin{pmatrix} j_1' & j_2' & J \\ 1/2 & -1/2 & 0 \end{pmatrix} \Big\} \tag{A.11}$$

for the scalar part of the quantity $G_J(j_1 j_2 j_1' j_2')$. The definition of the ratio Δ of radial matrix elements is given in equation (17).

In a similar way one gets for the spin-spin part

$$G_J^{SS}(j_1 j_2 j_1' j_2') = \frac{1}{16\pi} \sqrt{(2j_1+1)(2j_2+1)(2j_1'+1)(2j_2'+1)}\, R^{n_1 l_1 n_1' l_1'}_{n_2 l_2 n_2' l_2'}$$
$$\times \Big\{ (1-\Delta) \begin{pmatrix} j_1 & j_2 & J \\ 1/2 & 1/2 & -1 \end{pmatrix} \begin{pmatrix} j_1' & j_2' & J \\ 1/2 & 1/2 & -1 \end{pmatrix}$$
$$+ (-)^{l_2+l_2'+j_2+j_2'} [(2+\Delta)(1+(-)^{l_1+l_2+J}) - (1-\Delta)]$$
$$\times \begin{pmatrix} j_1 & j_2 & J \\ 1/2 & -1/2 & 0 \end{pmatrix} \begin{pmatrix} j_1' & j_2' & J \\ 1/2 & -1/2 & 0 \end{pmatrix} \Big\} \tag{A.12}$$

while the tensor part is given by the expression

$$G_J^T(j_1 j_2 j_1' j_2') = \frac{1}{8\pi} \sqrt{(2j_1+1)(2j_2+1)(2j_1'+1)(2j_2'+1)}\, R^{n_1 l_1 n_1' l_1'}_{n_2 l_2 n_2' l_2'}$$
$$\times (1-\Delta) \Big\{ \begin{pmatrix} j_1 & j_2 & J \\ 1/2 & 1/2 & -1 \end{pmatrix} \begin{pmatrix} j_1' & j_2' & J \\ 1/2 & 1/2 & -1 \end{pmatrix}$$
$$+ (-)^{l_2+l_2'+j_2+j_2'} (1-(-)^{l_1+l_2+J}) \begin{pmatrix} j_1 & j_2 & J \\ 1/2 & -1/2 & 0 \end{pmatrix} \begin{pmatrix} j_1' & j_2' & J \\ 1/2 & -1/2 & 0 \end{pmatrix} \Big\}. \tag{A.13}$$

The sum of these three terms, equation (A.11)–(A.13), should be introduced in equation (13).

References

[1] T. Hamada and I. D. Johnston, Nucl. Phys. *34*, 382 (1962).
[2] F. Tabakin, Ann. Phys. (N.Y.) *30*, 51 (1964).
[3] T. T. S. Kuo, Nucl. Phys. *A90*, 199 (1967).
[4] G. E. Brown and T. T. S. Kuo, Nucl. Phys. *A92*, 481 (1967).

[5] M. Baranger, Phys. Rev. *120*, 957 (1960).
[6] A. M. Lane, *Nuclear Theory* (Benjamin New York 1964).
[7] J. Hadermann and M. Simonius, Helv. phys. Acta *40*, 531 (1967).
[8] R. Arvieu and S. A. Moszowski, Phys. Rev. *145*, 830 (1966).
[9] E. Fermi, *Nuclear Physics* (University of Chicago Press 1963).
[10] L. Rosenfeld, *Nuclear Forces* (North-Holland Amsterdam 1948).
[11] J. D. Jackson and J. M. Blatt, Rev. Mod. Phys. *22*, 77 (1950).
[12] L. C. Biedenharn, J. M. Blatt and M. H. Kalos, Nucl. Phys. *6*, 359 (1958).
[13] J. Hadermann, Helv. phys. Acta *41*, 323 (1968).
[14] G. Vallois et al., Phys. Lett. *24B*, 512 (1967) and references cited therein.
[15] R. Tickle and J. Bardwick, Phys. Rev. *166*, 1167 (1968).
[16] V. Gillet et al., Nucl. Phys. *88*, 321 (1966).
[17] G. Muehllehner et al., Phys. Rev. *159*, 1039 (1967).
[18] J. M. Blatt and V. F. Weisskopf, *Theoretical Nuclear Physics* (Wiley, New York 1952).
[19] P. H. Stelson and L. Grodzins, Nuclear Data *A1*, 21 (1965).
[20] Nuclear Data Sheets.
[21] P. Weinzierl et al., Phys. Rev. *134*, B257 (1964).
[22] F. Schima et al., Phys. Rev. *132*, 2650 (1963).
[23] R. Arvieu et M. Veneroni, Phys. Lett. *5*, 142 (1963).
[24] A. Plastino, R. Arvieu and S. A. Moszkowski, Phys. Rev. *145*, 837 (1966).
[25] D. M. Clement and E. U. Baranger, Nucl. Phys. *89*, 145 (1966).
[26] W. W. True, Phys. Rev. *168*, 1388 (1968).
[27] J. M. Blatt and J. D. Jackson, Phys. Rev. *76*, 18 (1949).
[28] W. W. True and K. W. Ford, Phys. Rev. *109*, 1675 (1958).
[29] U. Götz and J. Hadermann, to be published.
[30] R. A. Edmonds, *Angular Momentum in Quantum Mechanics* (Princeton University Press 1957).
[31] S. G. Nilsson, Mat. Fys. Medd. Dan. Vid. Selsk. *29*, no. 16 (1955).
[32] A. de-Shalit, Phys. Rev. *91*, 1479 (1953).
[33] A. Arima et al., Progr. Theoret. Phys. *11*, 143 (1954).
[34] N. Stein and J. S. Lilley, Bull. Am. Phys. Soc. *10*, 497 (1965).
[35] P. Mukherjee and B. L. Cohen, Phys. Rev. *127*, 1284 (1962).
[36] F. P. Brady et al., University of California, Report No. CNL-UCD 23, 1964.